Advances in Radiation Oncology (2024) 9, 101634

advances in radiation oncology

www.advancesradonc.org

Scientific Article

Use of Virtual CT and On-Treatment MRI to Reduce Radiation Dose and Anesthesia Exposure Associated With the Adaptive Workflow in Pediatric Patients Treated With Intensity Modulated Proton Therapy

Khadija Sheikh, PhD,[a,b,*] Ryan Oglesby, PhD,[a] William T. Hrinivich, PhD,[a,b] Heng Li, PhD,[a,b] Matthew M. Ladra, MD,[a,b] and Sahaja Acharya, MD[a,b]

[a]*Department of Radiation Oncology and Molecular Sciences, Johns Hopkins University School of Medicine, Baltimore, Maryland; and* [b]*Department of Radiation Oncology, The Johns Hopkins Proton Center, Washington, District of Columbia*

Received 9 April 2024; accepted 5 September 2024

Purpose: The purpose of this study was to determine whether virtual computed tomography (vCT) derived from daily cone beam computed tomography (CBCT), or on-treatment magnetic resonance imaging (MRI_{tx}) can replace quality assurance computed tomography (qCT) in our clinical workflow to minimize imaging dose and potentially anesthesia exposure in patients requiring plan adaptation.

Methods and Materials: Pediatric patients (age <24 years) treated from 2020 to 2023 with intensity modulated proton therapy with at least 1 qCT during proton therapy were eligible. For cases that required plan adaptation, the dose was recalculated on vCT and compared with same-day qCT as well as the original planning computed tomography (pCT). Anatomic changes triggering plan adaptation were grouped into categories. Two pediatric radiation oncologists verified whether these changes could be detected using CBCT, qCT, and/or MRI_{tx}. A new adaptive imaging workflow was proposed to limit imaging dose and anesthesia exposure.

Results: One hundred sixty-eight pediatric patients were treated from 2020 to 2023. Across all patients, there were 517 qCT scans and 61 MRI_{tx} acquired. The median number of qCT scans per patient was 3 (range, 1-5). The treatment plans for 20 patients (12%) were adapted. In all patients requiring plan adaptation, there was a correlation between dose differences in target coverage and maximum body dose when comparing vCT with pCT and qCT with pCT ($n = 20$, $r^2 = 0.79$, $P < .01$, and $r^2 = 0.32$ $P = .01$, respectively). The most common reason for adaptation was tissue change (eg, inflammation, changes in abdominal gas, or diaphragmatic variability) in the beam path (10/20) and changes in tumor volume (6/20). All cases of weight change, tissue change in beam path, and unreproducible setup could be detected on CBCT. All cases of change in tumor volume within the brain were detected on MRI_{tx}. Replacing the qCT with the vCT was associated with an estimated median reduction of imaging dose by 50% and anesthesia exposure by 1.5 hours.

Conclusions: vCT derived from daily CBCT only or MRI_{tx} can safely replace qCT for monitoring dosimetric changes to trigger a new pCT in our clinical workflow. This change would potentially reduce imaging dose and anesthesia exposure.

Sources of support: This work had no specific funding.

Research data are stored in an institutional repository and will be shared upon request to the corresponding author.

*Corresponding author: Khadija Sheikh, PhD; Email: ksheikh4@jhmi.edu

https://doi.org/10.1016/j.adro.2024.101634

Introduction

Patients undergoing proton therapy often experience anatomic changes such as weight loss/gain, changes in tissue density, or tumor changes. These geometric changes may be treatment-related (eg, tumor shrinkage) or non-treatment-related, such as abdominal gas or mucosal filling of the sinuses. Because proton range is sensitive to tissue components in the beam path,[1] such changes in anatomy may result in a dose decrease in the clinical target volume and/or increase in dose to organs at risk (OAR), potentially increasing toxicity.[2] This necessitates adaptive replanning. As a result, higher plan adaptation rates are often seen for proton treatments compared with standard photon treatments.[3] For pediatric patients undergoing intensity modulated proton therapy (IMPT), adaptive proton therapy[4-6] can improve the delivered plan quality by systematically monitoring treatment variations (via daily onboard imaging or computed tomography [CT]/MRI scans acquired over the course of treatment) and reoptimizing the treatment plan to such variations early in the treatment.[7]

Cone beam CT (CBCT) has been used to generate proton dose estimation.[8-10] However, using CBCT for dose estimation and plan adaptation poses challenges because of inadequate CT number accuracy and image quality.[11] Consequently, quality assurance CTs (qCTs) acquired on the CT simulator during proton therapy are obtained to ensure the accuracy of dose delivery. On-treatment MRIs (MRI_{tx}) are also often acquired at the same time as qCTs as they are the modality of choice for visualizing most tumors treated with definitive radiation therapy.[12] The decision to initiate adaptive replanning is usually based on quantitative assessment of target coverage and OAR doses on the qCTs. However, this comes at a cost as qCTs not only require extra time from staff but also expose patients to additional imaging doses and potentially prolonged times under anesthesia, both (ie, dose and anesthesia) of which may be unnecessary if the patient does not require adaptation at that time.

Despite the growing use of proton therapy in pediatric cancers,[13-16] there are few recommendations for qCT frequency and adaptive planning workflow pertaining to pediatric cancers. At our institution, pediatric patients treated with IMPT undergo qCT scans to verify dose and identify cases that require adaptation because of anatomic changes. These patients also undergo daily CBCT. Here, we analyze qCT frequency with respect to the number and timing of plan adaptations to provide imaging recommendations for pediatric patients undergoing proton therapy with daily CBCT. We also determine when virtual CTs (vCT), derived from daily CBCT only, or MRI_{tx} can replace qCT to minimize imaging dose and potentially anesthesia exposure associated with the adaptive workflow across all pediatric disease sites included in this study.

Methods and Materials

Study subjects

The institutional review board at Johns Hopkins University approved this study. All pediatric patients treated at Johns Hopkins Proton Center who underwent IMPT with at least one qCT from 2020 to 2023 were included. One hundred sixty-eight pediatric patients (<24 years of age) were evaluated, including 20 patients requiring at least 1 adapted plan. pCTs and qCTs were acquired for treatment simulation using a 64 slice Definition Edge Plus fan-beam CT scanner (Siemens Healthineers) with 120 kV tube potential, modulated mAs, and 2 mm slice thickness with patients immobilized in the treatment position. All patients underwent pencil beam proton therapy on a Hitachi ProBeat (Hitachi Ltd) system using 2-4 treatment fields. The proton gantry-mounted CBCT system (Hitachi ProBeat, Hitachi Ltd) has a maximum field of view of 38 cm in the z-direction. The images were acquired in full-scan (179.9°-180°) or partial scan (45°-205°) mode at 100 kVp with resolutions ranging from 0.2 to 0.4 mm × 0.2 to 0.4 mm × 2 to 2.5 mm with an axial field of view of 20-37.5 cm and 69-145 number of slices, depending on the anatomic site.

The imaging protocol consisted of CT for treatment planning (pCT), daily gantry-mounted CBCT for patient setup, and qCTs acquired weekly or once every 2 weeks in the treatment position for verification during the treatment course. On-treatment MRIs were acquired using MAGNETOM Sola (Siemens Healthcare GmbH) for brain/craniospinal irradiation (CSI), spine, and abdomen/pelvis patients at the discretion of the attending physician, either during week 1, week 3, or midway through treatment. Patients were scanned in the treatment position.

Virtual CT generation

For this study, the vCTs were generated for 20 patients using the CBCTs acquired on the same day as the qCTs that triggered the adaptive plans. The vCT was defined as the deformed pCT to the anatomy of the CBCT. RayStation 2023B (RaySearch) was used to rigidly align the CBCT to the pCT by importing the registration created during the treatment session alignment. An algorithm for hybrid deformable image registration was used to deform the pCT to the CBCT, and no controlling regions of interest were used. The hybrid deformable image registration (DIR) algorithm known as ANACONDA ("anatomically constrained deformation algorithm") combines both anatomic information and image intensities.[17,18] This method was previously validated in lung cancer for CT-to-CT DIR and CT-to-CBCT DIR.[18,19] The vCT algorithm identifies

mismatched low-density regions between the reference pCT and a corrected CBCT.[20] This correction involves creating a joint histogram between the reference CT and CBCT, which generates a conversion function. A mask isolates anatomic differences, and a correction map is produced by smoothing these differences. The corrected CBCT is then obtained by adding this correction map.[21] Finally, mismatched air/lung regions in the pCT are replaced with values from the corrected CBCT to produce the vCT.

The dose was recomputed on the vCT using the original treatment plan. Similarly, the qCT acquired on the same day as the CBCT was rigidly registered to the pCT. The OAR contours were deformably and rigidly (depending on the treatment site) propagated onto the qCT and vCT. The targets were rigidly propagated on the qCT and vCT. All contours were evaluated and corrected accordingly by the dosimetrist and pediatric radiation oncologist. The treatment plan dose was recomputed onto the qCT.

Analysis

For each of the 20 patients, the dose distributions were compared between the vCT and qCT. First, 3D gamma analysis was performed comparing the vCT dose distribution with the qCT dose distribution. Three-dimensional gamma distributions were computed using Raystation. Two criteria of the distance to agreement and dose difference were evaluated (3%/3 mm, 3%/2 mm).[22] A 10% threshold of maximum dose was applied, and gamma pass rates were computed for the region within the body contour. Analysis was performed to determine whether the vCT was able to detect changes in dose distribution compared with the pCT similar to those detected by the qCT. We computed target coverage (clinical target volume covered by 95% of the prescription dose [V95%]) and body maximum dose (D_{max}) on the pCT, qCT, and vCT. Target coverage and body maximum doses were chosen as evaluation metrics to coincide with our clinical workflow when evaluating qCTs.

The criteria we use in the clinic to initiate plan adaptation include the evaluation of the robust evaluation. Briefly, each clinical plan is recomputed with ±3.5% range uncertainty and 3-5 mm (5 mm is used for thoracic and abdomen/pelvic sites) setup uncertainty in the left-right, superior-inferior, and anterior-posterior directions (resulting in 8 robustness scenarios, of which we evaluate the worst-case scenario dose). The robustness evaluation informs the lower limit of acceptable target coverage and upper limits of body/normal tissue maximum doses. When evaluating the qCT, if the target coverage is below the lower limit of robustness, a plan adaptation may be initiated. Similarly, if the upper limit of body/normal tissue maximum dose is exceeded when evaluating the recomputed dose on the qCT, a plan adaptation may be initiated. The target coverage and body maximum dose limits vary for each patient.

Given the different treatment sites, doses to OARs were not reported. The dose metric change detected by the qCT ($\Delta qCT[\%] = 100^*[D_{qCT}-D_{pCT}]/D_{pCT}$) and the vCT ($\Delta vCT[\%] = 100^*[D_{vCT}-D_{pCT}]/D_{pCT}$) was computed, as previously described.[23] Data were tested for normality using the Shapiro−Wilk normality test using SPSS v28.0 (IBM), and parametric tests were performed when the data satisfied normal distribution. Linear regression was performed between ΔqCT and ΔvCT using SPSS v28.0 (IBM). Line of best fit, Pearson correlation coefficients (r), Spearman correlations (r_s), and *P* values were computed to assess the statistical significance of the correlations.

Results

Study subjects

Twenty patients were included in the vCT analysis. Table 1 shows patient and tumor characteristics. The median age at radiation start was 8.4 years. Treatment sites included brain/CSI (54%), abdomen/pelvis (19%), thorax (11%), head and neck (10%), extremities (4%), and the spine (4%). Table E1 shows the summary of weekly on-treatment imaging for each patient with an adaptive plan and includes the number of fractions treated with the original plan.

Replanning rates and adaptive plans

In addition, Table 1 provides a summary of adapted patients and the number of qCTs acquired in adapted patients versus all patients. The patients requiring plan adaptation only required 1 adapted plan. The abdomen/pelvis site had the highest plan adaptation rate (7/31, 23%), followed by thorax (3/18, 17%) and extremity (1/7, 14%) sites. Sarcoma (rhabdomyosarcoma, Ewing's sarcoma, or other sarcoma) represented 8/20 (40%) of the adapted cases. For the entire study cohort and the adapted cohort, the mean number of qCTs acquired was 3, ranging from 1 to 5 qCTs acquired over the course of treatment.

Reasons for plan adaptation were reviewed and divided into 4 categories "weight change," "tissue change in the beam path," "tumor changes," and "set-up difficulties." "Weight change" included patients with an increase or decrease in body habitus not necessarily in the beam path. "Tissue changes in beam path" included patients who had developed edema/inflammation, consistent change in diaphragm position, or consistent change in bowel/rectal gas within the beam path. "Set-up difficulties" included a single patient with a nonreproducible and challenging setup. Specifically, a new mask had to be created because of the

Table 1 Patient and tumor characteristics

Characteristic	All patients (%)	Adapted patients (%)
Total number of patients	168	20
Total number of treatment courses		
First radiation course	168	20
Second radiation course	8	0
Age at radiation start (median)	8.4 y	9.8 y
Sex		
Female	79 (47)	13 (65)
Male	89 (53)	7 (35)
Tumor location		
Brain/CSI	90 (54)	7 (35)
Head and Neck	16 (10)	2 (10)
Thorax	18 (11)	3 (15)
Abdomen/Pelvis	31 (19)	7 (35)
Extremity	7 (4)	1 (5)
Spine	6 (4)	0 (0)
Tumor diagnosis		
Medulloblastoma	24 (14)	0 (0)
Rhabdomyosarcoma	23 (14)	4 (20)
High-grade Glioma	19 (11)	2 (10)
Ependymoma	17 (10)	2 (10)
Neuroblastoma	15 (9)	1 (5)
Ewing's Sarcoma	13 (8)	2 (10)
ATRT	6 (4)	0 (0)
Craniopharyngioma	4 (2)	1 (5)
CNS germ cell tumor	7 (4)	0 (0)
Hodgkin Lymphoma	6 (4)	2 (10)
Low-grade Glioma	5 (3)	0 (0)
Malignant rhabdoid tumor	2 (1)	1 (5)
Osteosarcoma	2 (1)	0 (0)
Non-CNS germ cell tumor	2 (1)	1 (5)
Other sarcoma	11 (7)	2 (10)
Other brain tumor	9 (5)	1 (5)
Other nonbrain/nonsarcoma tumor	3 (2)	1 (5)
Median number of qCTs per treatment course (range)	3 (1-5)	3 (1-5)

Abbreviations: ATRT = atypical teratoid rhabdoid tumor; CNS = central nervous system; qCT = quality assurance computed technology.

mobility of the C-Spine. Figure E1 shows the pCT, qCT, and same-day CBCT of patients requiring adaptive plans and provides an example of weight change (patient A), tissue change in beam path (patients B and C), and tumor changes (patient D). As shown in Table E2, the most common reason for adaptive planning was a tissue change in the beam path (10/20, 50%), followed by change in tumor (6/20, 30%) and change in weight (3/20, 15%). Changes in tumor were first caught on MRI_{tx} in week 1 or 3.

Virtual CTs

Representative dose distributions optimized on the pCT and recalculated on the qCT and vCT are shown in

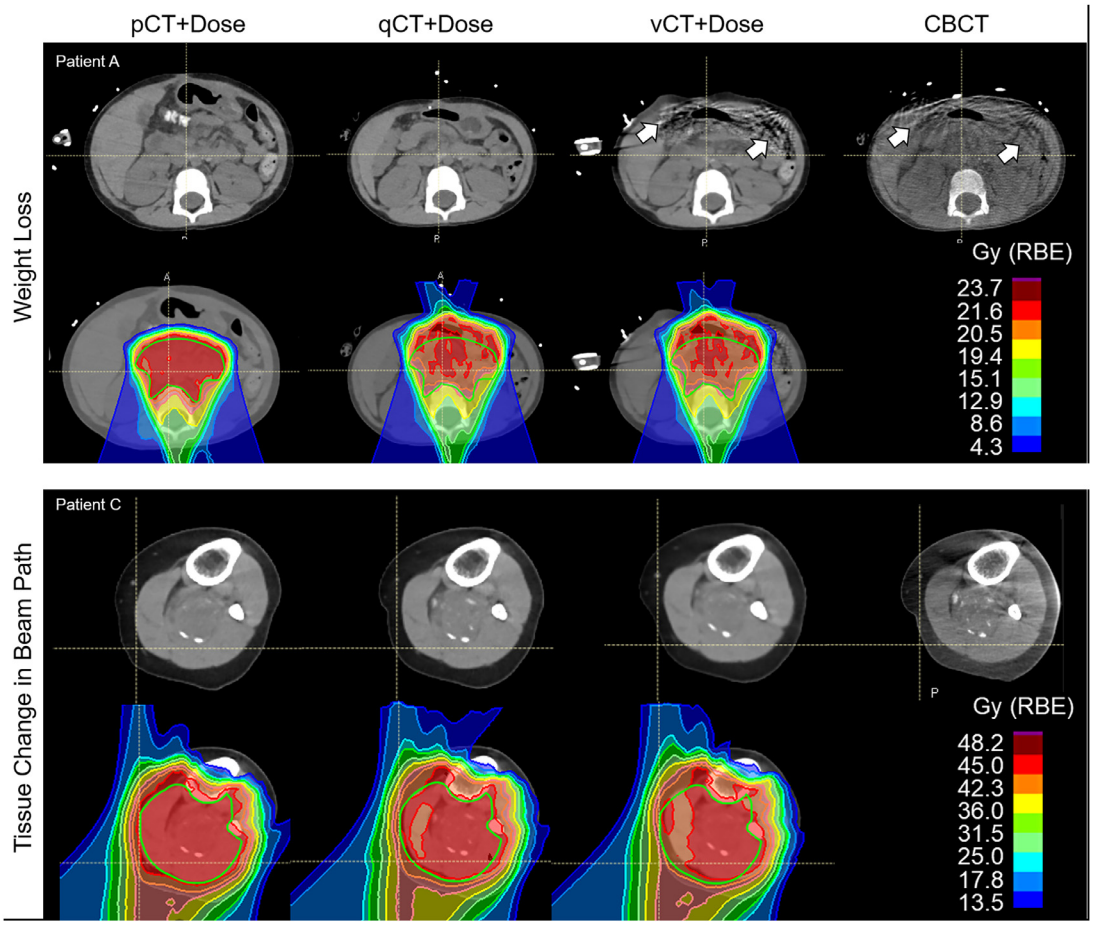

Figure 1 Representative dose distributions for 2 patients (illustrating weight loss on top and tissue changes in the beam path on the bottom) with the clinical target volume contoured in green. Planning computed technology (pCT), quality assurance computed technology (qCT), virtual computed technology (vCT) (generated from the cone beam computed technology [CBCT]), and same-day CBCT shown with corresponding doses. Note that the doses were recomputed on the qCT and vCT using the original treatment plan. Prescription isodose color wash is shown in red. White arrows indicate streaks in the vCT and CBCT.

Fig. 1. An example patient with weight loss (patient A) and tissue changes in the beam path (patient C) are shown. There are visual similarities between the dose distribution recomputed on the vCT and the qCT, where a drop in coverage can be observed in both patients A and C. It should be noted that the vCT and same-day CBCT show similarities in the air bubble in patient A; however, streaking artifacts are present in the anterior portion of the patient (white arrows). This is consistent with the notion that the vCT method in Raystation 2023b takes most of the image from the deformed CT, apart from low-density regions such as air/lung, which are taken from the corrected CBCT.[20]

Based on TG-218, 12 of 20 patients met the passing criteria for gamma analysis recommended for patient-specific plan quality assurance (3%/2 mm $\geq$ 90%).[22] Clinically, the passing rate is set to >95% at 3%/3 mm. Given these criteria, 16 of 20 patients had acceptable dose differences. Interestingly, the patients with lower pass rates included those with lesions in the thorax or abdomen/pelvis.

Figure 2 shows scatter plots of the change in dose recomputed using vCT (ΔvCT) versus the changes observed using the qCT (ΔqCT). The largest changes in target coverage were observed in the extremity and abdomen/pelvis patients, whereas the largest changes in body maximum doses were observed in the thorax and abdomen/pelvis cases. The correlation coefficient (P values) between qCTs and vCTs for changes detected in target coverage (Fig. 2A) and overall maximum dose (Fig. 2B) were $r_s = 0.91$ ($P < 0.01$) and $r = 0.57$ ($P = 0.01$). The slope of the line relating the changes in target coverage of 1.02 suggests that for every 1% change in coverage detected on the qCT, there is a 1.02% change detected on the vCT (ie, the vCT overestimates changes in target coverage compared with the qCT). In contrast, the slope of the line relating changes in body maximum dose of 0.88 suggests a slight underestimation in change detected on the vCT compared with the qCT. Taken together, these results suggest that caution must be taken when evaluating the doses recomputed on the

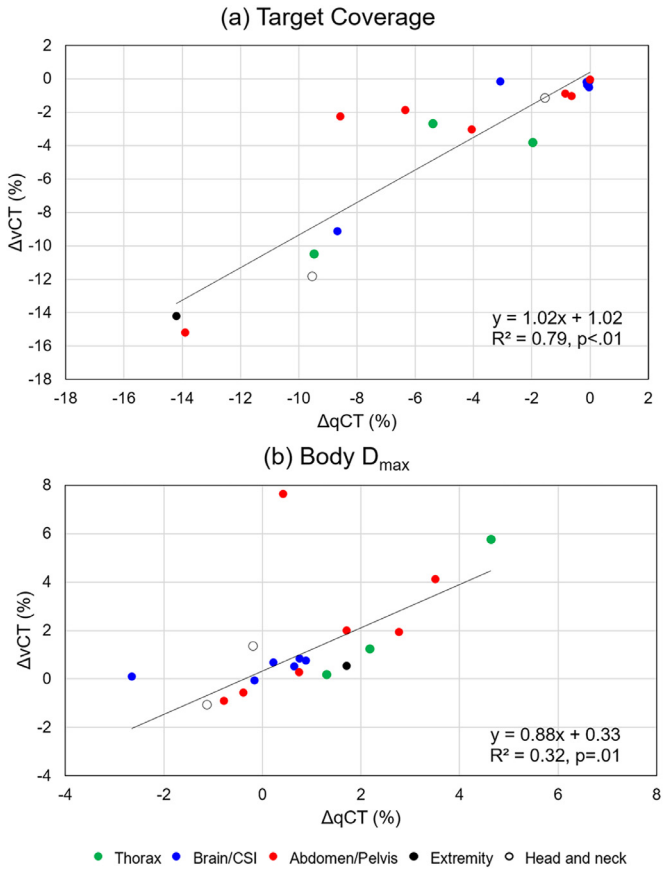

Figure 2 Scatter plots comparing dose metric changes detected using virtual computed technology (ΔvCT) to those detected using quality assurance computed technology (ΔqCT). Dose metric changes are computed relative to the original planning CT (pCT). The legend identifying the anatomic sites corresponding to colored markers is shown below.

vCT for patients with variations in air/low-density changes apparent on the CBCT. These patients may require a resimulation or a qCT to appropriately evaluate the body maximum doses.

Proposed workflow to limit qCTs

Figure 3 shows a scatter plot indicating in which week the anatomic changes were identified for the patients who underwent adaptation based on qCT. Most anatomic changes were observed on the qCT in the first week of treatment. Most changes were because of tissue changes in the beam path followed by weight changes. The abdomen/pelvis and thorax sites had the most changes observed in that first qCT. Fewer patients had observable changes on the second and third qCT. One brain patient (single blue square) had a challenging setup near the C-Spine, which warranted a resimulation in the third week of treatment. No plan adaptations were initiated using the qCTs acquired in weeks 4 and 5. Taken together, these results suggest that weekly qCTs may not be needed for all anatomic sites and that qCTs during weeks 1 or 2 may be able to capture significant changes.

The qCTs were evaluated based on the clinical goals set at the time of planning; these goals included target coverage, OAR dose limits, and body's maximum doses. Table E3 summarizes the frequency of anatomic or dosimetric changes detected on CBCT versus qCT versus MRI_{tx}. When the planned dose was recomputed on the qCT, 11 of 20 patients had clinical goals that warranted a plan adaptation. Specifically, these 11 patients had clinical goals (based on the recalculated dose on the qCT) that demonstrated either poor target coverage or a clinically unacceptable body maximum dose. In the remaining 9 patients, changes in dosimetry were not detected in the qCT; 6 patients had tumor changes caught on MRI, 1 patient had a challenging setup, and 2 patients were adapted because of physician preference (Table E3). Of the 20 patients who needed an adaptive plan, 14 had anatomic changes visible on the CBCT. All patients with a weight change, tissue changes in the beam path, and setup difficulties were caught on the CBCT. Patients with tumor changes were not caught on the CBCT or the qCT immediately, but on MRI_{tx}, where changes were visually

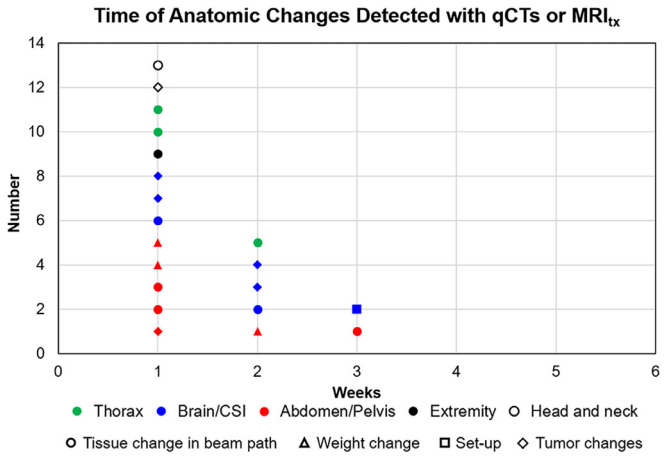

Figure 3 Scatter plot indicating when anatomic changes were identified for patients with tissue change in beam path (circle), weight change (triangle), and set-up concerns (square). Anatomic sites are indicated by color (ie, green: thorax, blue: brain/CSI, red: abdomen/pelvis, black: extremity, and white: head and neck). Most changes were identified at first quality assurance computed technology (qCT) during the first week of treatment. Two changes were identified at the third qCT for an abdomen/pelvis case with tissue changes in the beam path and a brain/CSI case that had a challenging setup and needed to be re-simulated. Changes in tumor were not identified with qCT.

apparent. It should be noted that these were brain/CSI patients who had scheduled MRI$_{tx}$. These results suggest that brain/CSI patients may benefit from MRI$_{tx}$ scans rather than qCTs.

Our previous workflow involved weekly qCTs for all pediatric sites, leading to 5 qCTs in patients with more than 25 fractions. Our new workflow results in a maximum of 2 qCTs (unless otherwise specified by the attending physician). Figure 4 outlines proposed workflows for brain/CSI, head and neck, and extremity (4A) and for abdomen/pelvis and thorax (4B) with the assumption that all patients have daily CBCT acquired and that they are reviewed by the treating physician. Table E4 summarizes our suggested on-treatment imaging frequency for qCTs, vCTs, and MRI$_{tx}$ for all sites. We recommend generating vCTs during weeks 1 and 3 of treatment for brain/CSI, head and neck, and extremity patients using daily CBCT. It is suggested that these patients also undergo MRI$_{tx}$ if indicated by the treating physician to evaluate for change in tumor. If an anatomic change is observed during daily CBCT review or dosimetric change is noted on the vCT, a new CT scan will be acquired, and a replan will be initiated using this newly acquired pCT. If the MRI$_{tx}$ shows changes in the target, a replan will be initiated on the original pCT. If no change is noted, the patient will continue treatment. For patients with abdomen/pelvis or thorax tumors, qCTs will be acquired in weeks 1 and 2 of treatment based on the frequency of replans that were observed during these time points. The second qCT will only be acquired in patients with more than 15 fractions. If an anatomic change is noted on the daily CBCT, a replan will be initiated on a qCT. If a dosimetric change is noted on the qCT, a replan will be initiated using that qCT. If changes are observed on the daily CBCT after the qCT shows changes, a new CT will be acquired. However, if no changes are observed, treatment may continue.

Imaging-related dose and anesthesia exposure

Under the new proposed workflow described above, patients with a tumor located in the brain/CSI, head and neck, or extremity would also undergo a qCT if it is triggered by a vCT or MRI$_{tx}$. Patients with tumors in the abdomen/pelvis or thorax would undergo 1 qCT during week 1 and 1 qCT during week 2. Assuming that the adaptation is triggered by a vCT leading to a qCT or a scheduled qCT during week 1 or 2, our new workflow would reduce the imaging dose associated with adaptive planning by a median of 50% (range, 0%-75%) (Table 2). Eight of the 20 adapted patients (40%) required anesthesia for imaging and treatment. Each qCT adds an hour of anesthesia exposure. By replacing the qCT with a vCT, we would reduce anesthesia exposure by a median of 1.5 hours (range, 0-3 hours) based on the 8 patients requiring anesthesia.

Discussion

In this study, we made the following observations: (1) patients with targets treated in the abdomen/pelvis or thorax had the highest rates of plan adaptation; (2) tissue change in beam path was the most common reason for plan adaptation; (3) dose recomputed on vCT data correlated with qCT data; (4) the decision to adapt the plan

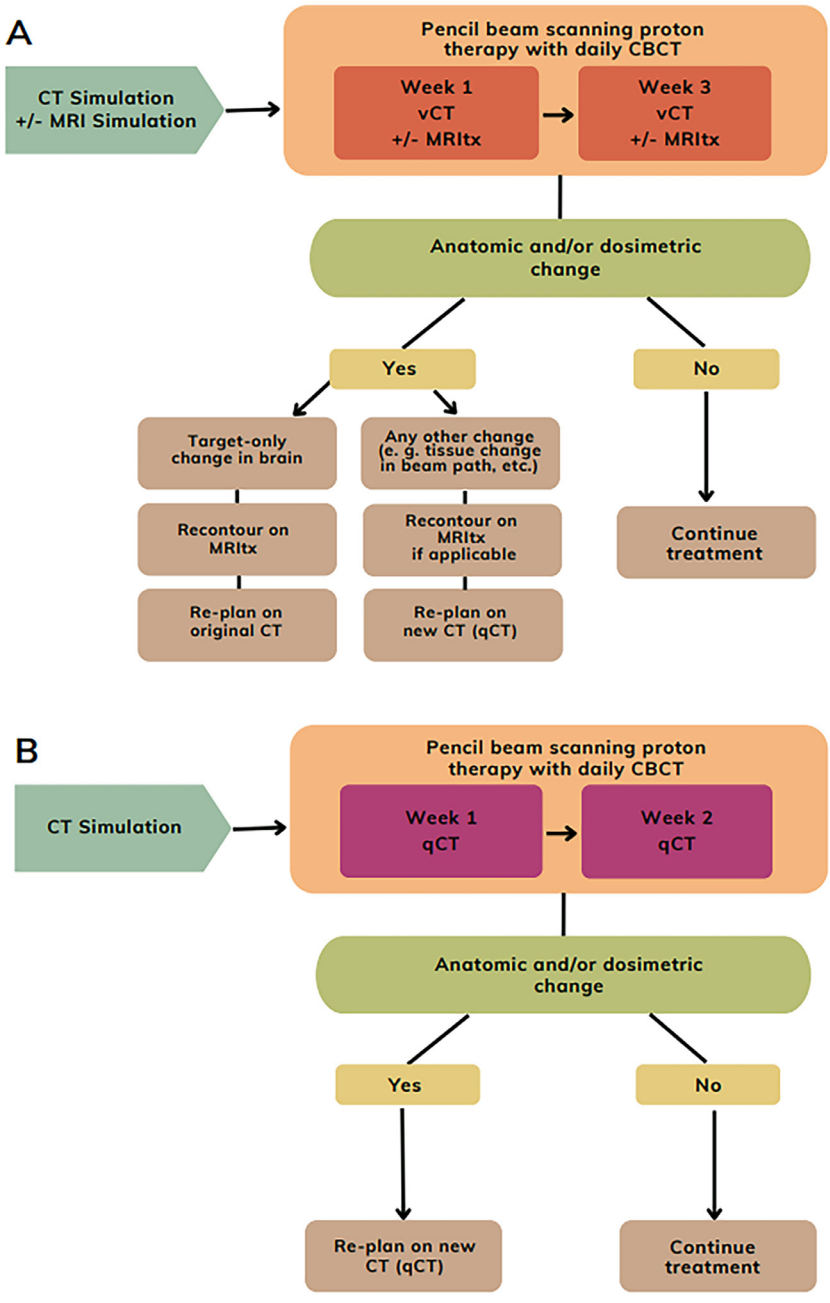

Figure 4 Proposed workflow for quality assurance computed technology (qCT) frequency and virtual computed technology (vCT) generation for (A) brain/CSI, head and neck, extremity and (B) abdomen/pelvis and thorax for patients with more than 15 fractions.

was made during the first 2 weeks of treatment and; (5) imaging dose and anesthesia exposure associated with the adaptive workflow can be minimized by replacing qCT with vCT. Based on these observations, we developed a workflow in our clinic to recommend omitting weekly or once every 2-week qCTs and implementing the generation of vCTs.

We reported 23% of our abdomen/pelvis cases requiring plan adaptations. This is unlike previous work that has suggested head and neck cancer patients undergoing proton therapy have the most frequent plan adaptation rate (~25%).[24] In our study, plan adaptations were mostly because of weight gain and changes in tissue within the beam path such as consistent gas in the bowel or rectum. In adult patients treated with proton therapy, rectal preparation is often performed using balloons, enemas, or anti-gas medication. This approach is challenging for pediatric patients, and the consistent presence of gas during treatment is often mitigated with an adaptive plan. Others[25] have proposed a "plan-of-the-day" approach where 2

Table 2 Reduction in radiation dose and anesthesia time with new adaptive workflow

Pt	Age (y)	qCTs old workflow	qCTs new workflow	Old workflow dose (mSv)	New workflow dose (mSv)	Dose difference (%)*	Anesthesia required†	Reduction in anesthesia (h)
1	2.5	4	2	16.58	8.29	−50	Yes	2
2	9.5	5	1	15.07	3.01	−80	No	NA
3	10.1	4	1	6.02	1.51	−75	No	NA
4	19.4	3	1	56.21	18.74	−67	No	NA
5	16.9	4	1	15.21	3.80	−75	No	NA
6	6.9	2	2	41.01	41.01	0	Yes	0
7	6.1	3	1	42.99	14.33	−67	Yes	2
8	4.1	4	2	6.30	3.15	−50	Yes	2
9	2.9	2	2	44.11	44.11	0	Yes	0
10	16.8	3	1	37.71	12.57	−67	No	NA
11	3.5	4	2	122.39	61.20	−50	Yes	2
12	14.3	1	1	6.20	12.40	0	No	NA
13	2.9	2	1	6.04	3.02	−50	Yes	1
14	7.8	1	1	1.35	2.70	0	No	NA
15	13.3	3	2	12.91	8.61	−33	No	NA
16	21.1	2	1	17.51	8.76	−50	No	NA
17	2.0	4	1	18.79	4.70	−75	Yes	3
18	12.7	5	2	40.34	16.13	−60	No	NA
19	16.3	2	2	11.14	11.14	0	No	NA
20	13.0	2	1	5.66	2.83	−50	No	NA

Number of qCTs acquired with old workflow and new workflow also indicated.
Abbreviations: h = hours; Pt = patient.
*Dose difference (%) refers to: (new workflow dose—the old workflow dose)/100.
†This assumes vCT replaces qCT. Each qCT adds an additional hour of anesthesia exposure.

plans are generated at the time of planning with various bladder fillings, which may be feasible for older pediatric patients. We also reported 17% of thoracic cases that required plan adaptations. This is not as high as previous studies reporting 60% of thoracic cancer patients requiring plan adaptations.[3,26,27] However, this is consistent with the notion that patients treated with lung cancer often undergo anatomic changes such as atelectasis, pleural effusion, and motion that lead to deviations in target coverage.

We also assessed the ability of the vCT to detect the same change in the dose as the qCT by computing dose metrics on the pCT, qCT, and vCT. Others have shown that qCTs agree with vCTs in regions of homogeneous tissues such as the brain and breast; however, notable discrepancies exist in the thorax and abdomen.[28] When we compared the dose distributions on the qCT with the vCT, with a gamma-index test using global 3%/2 mm criteria,[22] our pass rate was 90% across all patients who had an adaptive plan. This is lower than previously reported pass rates of 98% in pediatric head and neck cancer patients treated with proton therapy.[29] Our results suggest that although the vCT and qCT do not detect identical changes (especially in regions of heterogeneous media such as tissue-gas interfaces), the detected changes are strongly correlated such that a change detected on the vCT would be indicative of a similar change detected on the qCT. Although this result precludes the ability to use the vCT for direct quantitation or plan adaptation, it may be a valid approach to identify patients who require a qCT for quantitative dose assessment and potential plan adaptation.

Interestingly, most plan adaptations occurred following the first or second qCTs that occurred within the first 2 weeks of treatment. In fact, no plan adaptations occurred after the third week of treatment. This may have been because plan adaptations were not feasible so close to the end of treatment because they may take up to 5 days from the time of qCT to treatment. Therefore, weekly qCTs may not be warranted for pediatric patients undergoing proton therapy. In fact, most sites may only require 2 qCTs, 1 acquired during the first week of treatment and the second during the third week of treatment. This is consistent with previous findings in breast cancer, where a single qCT is sufficient to capture the majority of treatment-related changes when daily CBCT is being acquired.[30]

The benefit of reducing imaging dose and anesthesia exposure associated with the adaptive workflow should not be underappreciated. Although the dose associated with qCTs is small relative to the therapeutic radiation dose, young patients are particularly vulnerable to the late effects of radiation, and doses <2 Gy can have a potentially meaningful effect on certain functions such as fertility.[31,32] Furthermore, prolonging anesthesia exposure is associated with a greater risk of neurocognitive deficits in young children.[33]

We developed a new workflow for performing qCTs for pediatric patients treated with IMPT and daily CBCTs. We are in the process of implementing this workflow into our clinic and have since removed the requirement to acquire weekly qCTs. It is important to note that all weight/tissue changes could be identified on the daily CBCT; however, tumor changes could only be identified using MRI_{tx}. Consequently, we recommend omitting weekly qCTs for all sites and adding MRI_{tx} for brain/CSI sites. This is similar to previous work in pediatric parameningeal rhabdomyosarcoma that suggested qCTs to be acquired during weeks 1 and 2-3 of treatment to account for tumor regression.[34] We propose acquiring 2 qCTs over the course of treatment for thorax and abdomen/pelvic cases because of limitations in the generation of vCT near air-tissue interfaces. The first qCT is recommended to be acquired within the first week of treatment, and the second qCT is recommended to be acquired in the second week of treatment. We also propose using daily CBCTs to generate vCTs for brain cases in the first and third weeks of treatment. In the early stage of clinical implementation, it will be critical to conduct a visual inspection of the daily CBCTs and the vCT image quality. We do not recommend generating vCTs for cases where the CBCT does not encompass the entire path of the beam. Because the proton dose calculation depends critically on accurately modeling all tissue in the beam path, any occlusion of tissue in the CBCT prevents the generation of a vCT for dose calculation.

Taken together, this work provides recommendations for adaptive workflow for pediatric patients treated with IMPT. Anatomic changes prompting adaptation can be identified on CBCT if related to weight change, tissue change in beam path, and unreproducible setup. Daily CBCT further allows the generation of vCTs that can replace weekly qCTs and trigger plan adaptation. Target-related changes can be identified on MRI_{tx}, thus omitting the need for weekly or once every 2-week qCTs.

Disclosures

William T. Hrinivich discloses grant funding from Varian Medical Systems.

Acknowledgments

We would like thank Dhara Vyas, BS, for her administrative assistance. Khadija Sheikh was responsible for statistical analysis.

Supplementary materials

Supplementary material associated with this article can be found in the online version at doi:10.1016/j.adro.2024.101634.

References

1. Engelsman M, Schwarz M, Dong L. Physics controversies in proton therapy. *Semin Radiat Oncol*. 2013;23:88-96.
2. Arjomandy B. Evaluation of patient residual deviation and its impact on dose distribution for proton radiotherapy. *Med Dosim*. 2011;36:321-329.
3. Hoffmann L, Alber M, Jensen MF, Holt MI, Møller DS. Adaptation is mandatory for intensity modulated proton therapy of advanced lung cancer to ensure target coverage. *Radiother Oncol*. 2017;122:400-405.
4. Yan D, Vicini F, Wong J, Martinez A. Adaptive radiation therapy. *Phys Med Biol*. 1997;42:123-132.
5. Hui Z, Zhang X, Starkschall G, et al. Effects of interfractional motion and anatomic changes on proton therapy dose distribution in lung cancer. *Int J Radiat Oncol Biol Phys*. 2008;72:1385-1395.
6. Koay EJ, Lege D, Mohan R, Komaki R, Cox JD, Chang JY. Adaptive/nonadaptive proton radiation planning and outcomes in a phase II trial for locally advanced non-small cell lung cancer. *Int J Radiat Oncol Biol Phys*. 2012;84:1093-1100.
7. Acharya S, Wang C, Quesada S, et al. Adaptive proton therapy for pediatric patients: improving the quality of the delivered plan with on-treatment MRI. *Int J Radiat Oncol Biol Phys*. 2021;109:242-251.
8. Uh J, Wang C, Acharya S, Krasin MJ, C-Ho Hua. Training a deep neural network coping with diversities in abdominal and pelvic images of children and young adults for CBCT-based adaptive proton therapy. *Radiother Oncol*. 2021;160:250-258.
9. Kurz C, Dedes G, Resch A, et al. Comparing cone-beam CT intensity correction methods for dose recalculation in adaptive intensity-modulated photon and proton therapy for head and neck cancer. *Acta Oncol*. 2015;54:1651-1657.
10. Kurz C, Kamp F, Park YK, et al. Investigating deformable image registration and scatter correction for CBCT-based dose calculation in adaptive IMPT. *Med Phys*. 2016;43:5635-5646.
11. Yang M, Zhu XR, Park PC, et al. Comprehensive analysis of proton range uncertainties related to patient stopping-power-ratio estimation using the stoichiometric calibration. *Phys Med Biol*. 2012;57:4095-4115.
12. Khoo VS, Joon DL. New developments in MRI for target volume delineation in radiotherapy. *Br J Radiol*. 2006;79:S2-15.
13. Ladra MM, Edgington SK, Mahajan A, et al. A dosimetric comparison of proton and intensity modulated radiation therapy in pediatric rhabdomyosarcoma patients enrolled on a prospective phase II proton study. *Radiother Oncol*. 2014;113:77-83.
14. Wong RX, Faught J, Gargone M, et al. Cardiac-sparing and breast-sparing whole lung irradiation using intensity-modulated proton therapy. *Int J Part Ther*. 2021;7:65-73.
15. Bischoff M, Khalil DA, Frisch S, et al. Outcome after modern proton beam therapy in childhood craniopharyngioma: results of the

prospective registry study KiProReg. *Int J Radiat Oncol Biol Phys*. 2024;120:137-148.
16. Ravindra VM, Okcu MF, Ruggieri L, et al. Comparison of multimodal surgical and radiation treatment methods for pediatric craniopharyngioma: long-term analysis of progression-free survival and morbidity. *J Neurosurg Pediatr*. 2021;28:152-159.
17. RayStation. *Deformable Registration in Raystation (White Paper)*. 2017. https://www.raysearchlabs.com/media/whitepapers/.
18. Weistrand O, Svensson S. The ANACONDA algorithm for deformable image registration in radiotherapy. *Med Phys*. 2015;42:40-53.
19. Kadoya N, Nakajima Y, Saito M, et al. Multi-institutional validation study of commercially available deformable image registration software for thoracic images. *Int J Radiat Oncol Biol Phys [Internet]*. 2016;96:422-431.
20. Raystation. *Synthetic CT Generation in Raystation for Enhanced Workflows in Adaptive Radiotherapy (Whitepaper)*. 2023. https://www.raysearchlabs.com/siteassets/media/publications/white-papers/wp-pdfs/synthetic_ct_whitepaper.pdf.
21. RaySearch Laboratories. *RAYSTATION 2023B: Reference Manual*. Stockholm; 2023.
22. Miften M, Olch A, Mihailidis D, et al. Tolerance limits and methodologies for IMRT measurement-based verification QA: recommendations of AAPM task group no. 218. *Med Phys*. 2018;45:e53-e83.
23. Sheikh K, Liu D, Li H, Acharya S, Ladra MM, Hrinivich WT. Dosimetric evaluation of cone-beam CT-based synthetic CTs in pediatric patients undergoing intensity-modulated proton therapy. *J Appl Clin Med Phys*. 2022;23:e13604.
24. Trnkova P, Zhang Y, Toshito T, et al. A survey of practice patterns for adaptive particle therapy for interfractional changes. *Phys Imaging Radiat Oncol*. 2023;26: 100442.
25. van de Schoot AJAJ, de Boer P, Crama KF, et al. Dosimetric advantages of proton therapy compared with photon therapy using an adaptive strategy in cervical cancer. *Acta Oncol (Madr)*. 2016; 55:892-899.
26. Møller DS, Khalil AA, Knap MM, Hoffmann L. Adaptive radiotherapy of lung cancer patients with pleural effusion or atelectasis. *Radiother Oncol*. 2014;110:517-522.
27. Britton KR, Starkschall G, Liu H, et al. Consequences of anatomic changes and respiratory motion on radiation dose distributions in conformal radiotherapy for locally advanced non-small-cell lung cancer. *Int J Radiat Oncol Biol Phys*. 2009;73:94-102.
28. Tsai P, Tseng YL, Shen B, et al. The applications and pitfalls of cone-beam computed tomography-based synthetic computed tomography for adaptive evaluation in pencil-beam scanning proton therapy. *Cancers (Basel)*. 2023;15:5101.
29. Bäumer C, Frakulli R, Kohl J, et al. Adaptive proton therapy of pediatric head and neck cases using MRI-based synthetic CTs: initial experience of the prospective KiAPT study. *Cancers (Basel)*. 2022;14:2616.
30. Ger RB, Sheikh K, Gogineni E, et al. Planning and treatment recommendations for breast proton therapy from a single center's experience. *Adv Radiat Oncol*. 2023;8: 101069.
31. Baliga S, Patel S, El Naqa I, et al. Testicular dysfunction in male childhood cancer survivors treated with radiation therapy: a PENTEC comprehensive review. *Int J Radiat Oncol Biol Phys*. 2023; 119:610-624.
32. Hill-Kayser C, Yorke E, Jackson A, et al. Effects of radiation therapy on the female reproductive tract in childhood cancer survivors: a PENTEC comprehensive review. *Int J Radiat Oncol Biol Phys*. 2024; 119:588-609.
33. Jacola LM, Anghelescu DL, Hall L, et al. Anesthesia exposure during therapy predicts neurocognitive outcomes in survivors of childhood medulloblastoma. *J Pediatr*. 2020;223:141-147.e4.
34. Uh J, Jordan JA, Pappo AS, Krasin MJ, Hua C. Adaptive proton therapy for pediatric parameningeal rhabdomyosarcoma: on-treatment anatomic changes and timing to replanning. *Clin Oncol (R Coll Radiol)*. 2023;35:245-254.